Available online at www.sciencedirect.com
SCIENCE DIRECT
Journal of Molecular Graphics and Modelling 24 (2006) 465–474
Journal of Molecular Graphics and Modelling
www.elsevier.com/locate/JMGM

Flap opening mechanism of HIV-1 protease

Gergely Tóth [a,*], Attila Borics [b]

[a] Locus Pharmaceuticals, Four Valley Square, 512 Township Line Rd., Blue Bell, PA 19422, USA
[b] Department of Biomedical Sciences, Creighton University Medical Center, Omaha, NE 68178, USA

Received 22 June 2005; received in revised form 22 August 2005; accepted 23 August 2005
Available online 26 September 2005

Abstract

The active site of aspartic proteases, such as HIV-1 protease (PR), is covered by one or more flaps, which restrict access to the active site. For HIV-1 PR, X-ray diffraction studies suggested that in the free enzyme the two flaps are packed onto each other loosely in a semi-open conformation, while molecular dynamics (MD) studies observed that the flaps can also separate into *open* conformations. In this study, the mechanism of flap opening and the structure and dynamics of HIV-1 PR with semi-open and open flap conformations were investigated using molecular dynamics simulations. The flaps showed complex dynamic behavior as two distinct mechanisms of flap opening and various stable flap conformations (semi-open, open and curled) were observed during the simulations. A network of weakly polar interactions between the flaps were proposed to be responsible for stabilizing the semi-open flap conformation. It is hypothesized that such interactions could be responsible for making flap opening a highly sensitive gating mechanism which control access to the active site.

Keywords: HIV-1 protease; Flap opening; Weakly polar interaction; Molecular dynamics

1. Introduction

Human immunodeficiency virus type 1 protease (HIV-1 PR) cleaves the *gag* and *pol* viral polyproteins in the maturation step during the replication cycle of the virus. Inhibition of HIV-1 PR prevents the virus from taking its mature and infectious form, and therefore it cannot replicate itself [1]. Seven commercially available drugs are based on the inhibition of this enzyme to treat acquired immune deficiency syndrome (AIDS) [2]. The clinical success of these drugs is hindered by the frequent occurrence of drug-resistant mutations of the HIV-1 PR. It is estimated, that in 2003 the AIDS epidemic claimed three million lives and five million people acquired HIV, raising the number of infected people globally to 40 million. Therefore, the need for the complete understanding of the structure and dynamics of the HIV-1 PR relating to enzymatic activity and inhibitor design is very significant.

The active site of aspartic proteases is characteristically covered by flaps, which restrict access to the active site (Fig. 1). HIV-1 PR, a member of the aspartyl protease family of enzymes, is a homodimer, with the functional Asp residues located at the dimer interface. The active site of HIV-1 PR is covered by two flaps, flexible antiparallel β-sheets, consisting of residues 45–55. X-ray diffraction studies [3–5] showed that in the free enzyme the flaps are packed onto each other loosely in a *semi-open* conformation, and the overall structure of the enzyme is less compact compared to the crystal structure of the inhibitor bound protease [6,7]. Recent NMR studies of the ligand free HIV-1 PR showed that the flap region can move on a sub-microsecond time scale, while the Gly-rich flap tips are more flexible, moving on sub-nanosecond time scale [8–11]. Interestingly, the flaps are reversed into a *closed* conformation in the ligand bound protease compared to the ligand free enzyme, which suggests that an extensive conformational change takes place upon ligand binding [5,12,13] (Fig. 1). Molecular dynamics (MD) simulations [14–16] of HIV-1 PR proposed that flap separation into *open* flap conformation could occur in the absence of ligand at 300 K temperature [17] or due to a small external impulse on the flaps [18]. An investigation of the free HIV-1 PR enzyme in solution state by NMR spectroscopy found that this semi-open conformation is dominant at 298 K, but did not dismiss the possibility of the existence of open and closed conformers with a significantly lower population [9].

Crystal structures of some other retroviral aspartic proteases suggest the possibility of alternate flap conformations in the ligand free state. The crystal structures of the ligand free simian

* Corresponding author. Tel.: +1 6503242560.
E-mail address: gergely.toth@gmail.com (G. Tóth).

1093-3263/$ – see front matter © 2005 Elsevier Inc. All rights reserved.
doi:10.1016/j.jmgm.2005.08.008

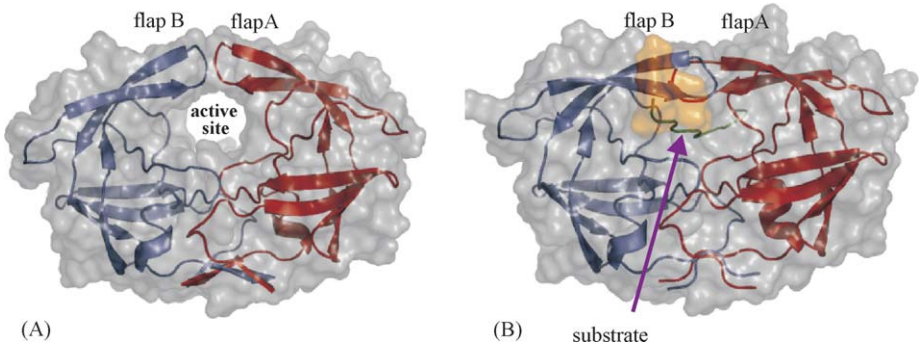

Fig. 1. Surface representation of (A) substrate free and (B) substrate bound structure of HIV-1 PR. Monomer A, monomer B and substrate are in red, blue and green cartoon drawing, respectively. The surface of HIV-1 PR is gray while the surface of the substrate is in orange representation.

immunodeficiency virus protease contains both closed [19] and open-like [20] flap conformations. It has been also suggested that crystal packing and crystallization conditions may affect the conformations of the flaps in crystal structures of aspartic proteases. In the case of HIV-1 PR, tetragonal crystals of the ligand free protease resulted in semi-open flap conformation [3–5] while hexagonal crystals of ligand free tethered HIV-1 PR carrying an asymmetric mutation C95M in one subunit of the dimer [21] protease resulted the closed conformation [21]. It was proposed that HIV-1 PR can adopt open flap conformations, if not prevented by crystal packing contacts. Freedberg and co-workers [9] reported a detailed analysis and comparison between NMR and MD results of the flap dynamics of the ligand free HIV-1 PR. They suggested on the bases of their NMR studies and the MD results of Scott and Schiffer [17] and Collins et al. [18] that the flaps may exist in an ensemble of conformations ranging between the semi-open and open conformations. In addition, they pointed out that structures resembling the open conformations of the flaps have not been observed experimentally before in the wild type of HIV-1 PR.

In contrast to the open conformation, free access to the active site of HIV-1 PR is sterically restricted in the semi-open conformation. This led to a model for the binding mechanism of the substrate to HIV-1 PR, in which first the ligand binds into the active site of the protease with open flap conformation, and next the flaps extend over the substrate and allow proteolysis to occur [17,18].

Our study explores flap dynamics and the mechanism of flap opening in atomic detail by studying the flap–flap interactions in ligand free HIV-1 PR at different temperatures using MD simulations. For the first time, the structural nature of flap–flap interactions and their function in flap opening is described. Moreover, the role of flap opening and flap dynamics in ligand binding mechanism of HIV-1 PR is discussed.

2. Methodology

Calculations were performed on eight AMD Athlon MP 2400+ computer nodes, in internal coordinate space (only torsion angles were considered while bond length and bond angles were set rigid) using the Imagiro molecular mechanics program [22] (Imagiro was developed at Protein Mechanics, CA, USA and at Locus Pharmaceuticals, PA, USA) and the OPLS-AA [23] molecular force field with GB/SA implicit solvation [24]. The OPLS-AA force field was projected into internal coordinates using a scheme similar to one recently proposed [25]. The crystal structure of the ligand free HIV-1 PR (pdb access code: 1hhp) [3] was used as starting structure for the calculations. Initially, the system was subjected to energy minimization utilizing dynamic relaxation [26]. The energy minimized structure of the ligand free HIV-1 PR served as input for Langevin dynamics simulations. Simulations were performed with the system's temperature set to 296, 301, 306, 311, 316 and 321 K for 5, 5, 2.2, 5, 5 and 1 ns, respectively, to provide slightly different simulation conditions. An error controlled, adaptive time step integrator, Runge–Kutta–Merson [27], was used to integrate Newton's equation of motion, with an average time step of approximately 9 fs. Such integration time steps were possible, because high frequency motions from bond stretching and angle bending were not present during the simulation of the protein in internal coordinate space. The size of integration time steps was ultimately limited by the frequency of dihedral angle motions and atom collisions (Lennard–Jones "rattling"). The frictional coefficient used in LD was set to 2 ps^{-1}, in order to facilitate the observation of otherwise slow, large-scale motions in a reasonable time frame [28]. In order to model the flap–flap interactions the most realistically no cutoffs were used for the calculations of non-bonded interactions.

To identify interactions between an aromatic ring of a residue and the hydrogen of a C–H_n group (CH$\cdots\pi$ interactions), the NMR ring shift (σ_{ring}) of the hydrogens of the C–H_n groups was calculated. The σ_{ring} value is influenced by the proximity and orientation of the aromatic ring. Interacting groups with σ_{ring} of -0.25 ppm or lower are considered to contain CH$\cdots\pi$ interactions [29,30]. The Total program [31] was used to calculate σ_{ring}. Interactions between C–H of either the aromatic rings or C_α–H and backbone carbonyl groups ($C_{AR}H\cdots O{=}C$, $C_\alpha H\cdots O{=}C$) were assigned when the distance between the hydrogen of the C–H group and the oxygen of the C–O group was less than 3.0 Å, the distance between the carbon of the C–H group and the oxygen of the C–O group was less than 3.8 Å and when the angle C–H$\cdots$O was larger than 95° [32].

All figures showing molecular structure were generated using the PyMOL program [33]. Furthermore, PyMOL was used for the visual inspection of HIV-1 PR with various flap conformations in surface representation mode.

3. Results

3.1. Flap conformations observed during the trajectories

The stability of the semi-open flap conformation can be monitored by measuring the distance between I50A C_α and I50B C_α located on the tip of the flaps [18]. Fig. 2 shows the evolution of this distance during the simulations. In the simulation at 296 and 316 K the flaps stayed in the semi-open conformation, at 301, 306, and 321 K the flaps separated into open conformations, and at 311 K the flaps separated and then they approached each other again as their tips curled into the active site of HIV-1 PR. In the semi-open flap conformation the distance between the C_α atoms of I50A and I50B was measured to be about 6 Å during the trajectories. The distance between I50A C_α and I50B C_α in open flap conformations was between 10 and 32 Å, while in the curled flap conformations this distance was around 5 Å. These calculations indicate that the flaps may exist in a complex ensemble of conformations during the simulations ranging between semi-open and open conformations (Fig. 3).

3.2. Dynamics of the semi-open flap conformation

The simulations at 296 and 316 K sampled conformational states around the semi-open conformation of the HIV-1 PR flaps. The flaps showed the highest structural fluctuation and mobility during the simulations (Fig. 4: RMSD for the simulation of 316 K was similar and thus this data is not shown). Throughout the simulation, the flaps remained in their semi-open conformations and did not separate. The distance between the C_α atoms of I50A and I50B is 4.91 Å in the crystal structure of the ligand free HIV-1 PR, while

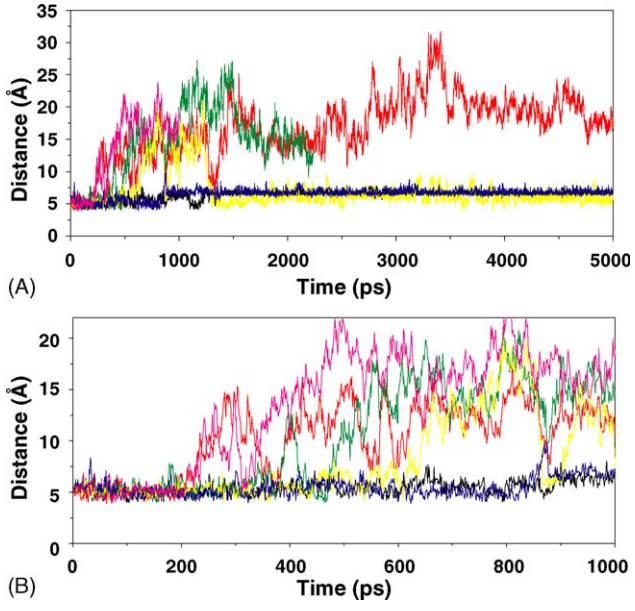

Fig. 2. The evolution of the distance during the simulations between the C_α atom of I50A and the C_α atom of I50B at 296 K (black line), at 301 K (red line), at 306 K (green line), at 311 K (yellow line), at 316 K (blue line) and at 321 K (purple line). Time scales: 0–5000 ps (A) and 0–1000 ps (B).

Table 1
Weakly polar interactions observed during the simulation at 296 and 316 K of ligand free HIV-1 PR in semi-open flap conformation

$C_\alpha H\cdots O{=}C$	$C_{AR}H\cdots O{=}C$	$CH\cdots\pi$
I50B $H_{C\alpha}$–G49A $O_{C=O}$	G51B $O_{C=O}$–F53A $H_{\delta1}$	I50A $H_{\delta1}$–F53A
I50A $H_{C\alpha}$–G49B $O_{C=O}$	G51A $O_{C=O}$–F53A $H_{\varepsilon2}$	I50B $H_{\delta1}$–F53B
	G51A $O_{C=O}$–F53B $H_{\varepsilon1}$	I50B $H_{\gamma1}$–F53A
	G51A $O_{C=O}$–F53B $H_{\varepsilon2}$	G48A $H_{\alpha1}$–F53B
	G51A $O_{C=O}$–F53B H_{ζ}	G48B $H_{\alpha1}$–F53A
		G48B $H_{\alpha2}$–F53A

average distances of 6.38 ± 0.69 and 6.54 ± 0.74 Å were observed in the simulations at 296 and 316 K, respectively. During both simulations the side chain of I50A formed a hydrophobic cluster with P81B as flap A shifted toward the loop made up of residues 79–83 of monomer A. This caused the initially symmetric semi-open flap conformation to become asymmetric (Fig. 5) as the position of the flap–flap contacts slightly shifted from being above and in the middle of the active site toward being above and in the side of the active site. This shift can be monitored during the trajectories by the proximity of the side chains of I50A and P81A using the distance between the C_β atom of I50 and C_γ atom of P81 (Fig. 6). Although, the existence of the hydrophobic cluster between I50A and P81B was metastable, the side chains of these two residues stayed in the proximity of each other during both simulations. The average distances between the C_β atom of I50A and the C_γ atom of P81A during the trajectories at 296 and 316 K were 8.87 ± 1.87 and 6.25 ± 1.63 Å, respectively.

The nature of the flap–flap interaction was investigated in detail in the simulation done at 296 and 316 K. It was found that no conventional hydrogen bonds exist between flap A and flap B in the semi-open conformation of the flaps in the crystal structure, however, weakly polar interactions [34,35], $CH\cdots O{=}C$ [32,36] and $CH\cdots\pi$ [37] interactions, were identified between the two flaps (Fig. 7). We propose that these weakly polar interactions between the flaps are

Table 2
Calculated σ_{ring} of selected hydrogens in the flaps in the crystal structure (pdb access code: 1hhp) and during the simulation at 296 K

Monomer A		Monomer B	
Atom	σ_{ring}[a]	Atom	σ_{ring}[a]
X-ray			
G48A HA1	−1.08	G48B HA1	−1.08
G48A HA2	−0.61	G48B HA2	−0.61
G49A NH	−0.37	G49B NH	−0.37
I50A HD1	−0.75	I50B HD1	−0.75
I50A HG1	−0.13	I50B HG1	−0.13
MD			
G48A HA1	-0.22 ± 0.34	G48B HA1	-0.42 ± 0.46
G48A HA2	-0.33 ± 0.38	G48B HA2	-0.27 ± 0.32
G49A NH	-0.23 ± 0.12	G49B NH	-0.29 ± 0.14
I50A HD1	-0.05 ± 0.21	I50A HD1	-0.04 ± 0.14
I50A HG1	-0.06 ± 0.10	I50B HG1	-0.38 ± 0.36

[a] σ_{ring} in ppm.

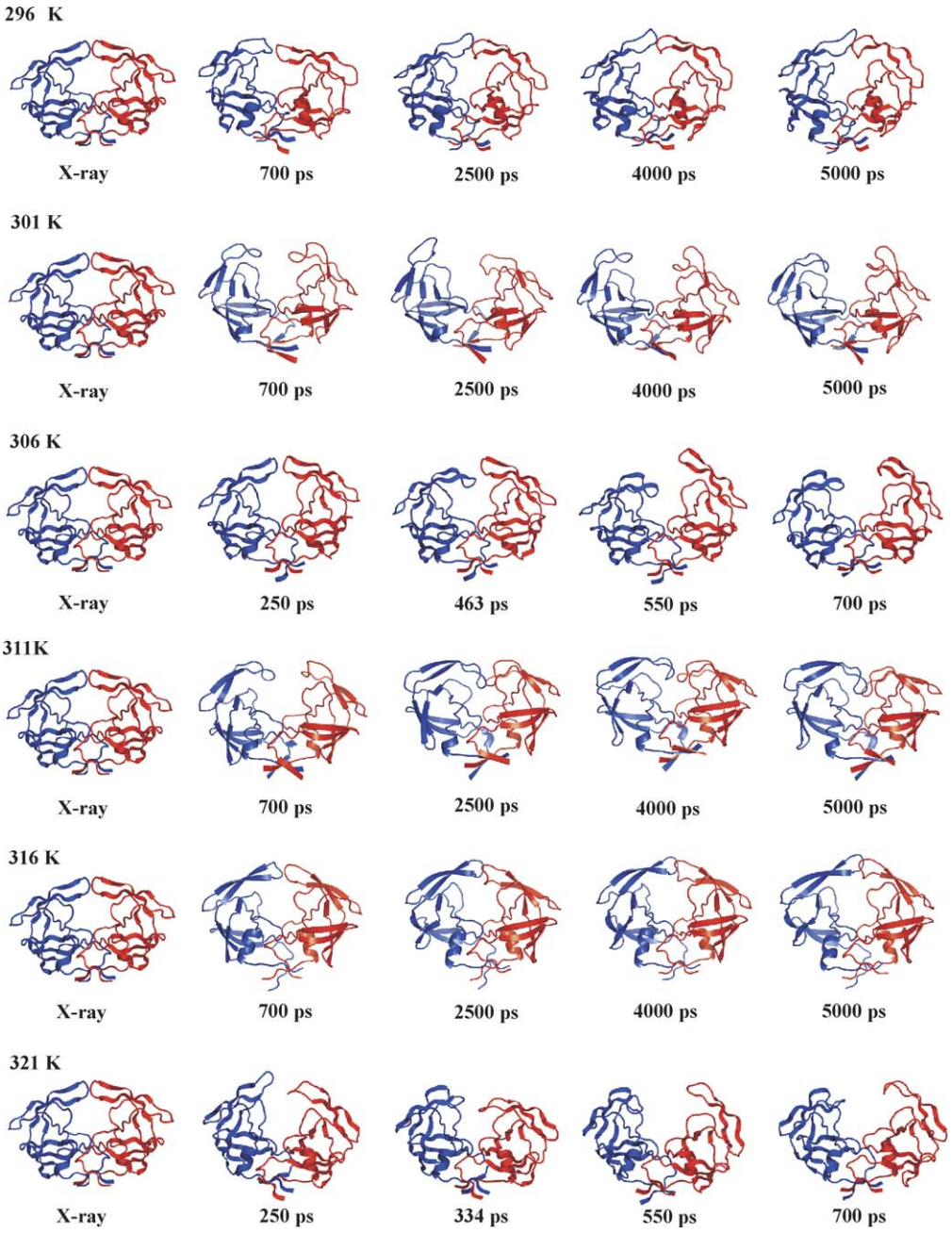

Fig. 3. Cartoon drawing of snapshots showing the evolution of the structures of HIV-1 PR during the trajectories at 296, 301, 306, 311, 316 and 321 K. Monomer A is in red, while monomer B is in blue.

responsible for the stability of the semi-open flap conformations of HIV-1 PR during the simulations.

The presence of these interactions was monitored throughout both trajectories (Table 1). Here we provide details for the simulation at 296 K. (Similar weakly polar interactions were detected for the simulation of 316 K (Table 1), thus this data is not discussed.) In the first 1400 ps, $C_{\alpha}H\cdots O{=}C$ interactions existed between I50B $H_{C\alpha}$ and G49A $O_{C{=}O}$, and I50A $H_{C\alpha}$ and G49B $O_{C{=}O}$ (Fig. 8A). $C_{AR}H\cdots O{=}C$ interactions existed between G51A $O_{C{=}O}$ and F53B $H_{\varepsilon 1}$, G51A $O_{C{=}O}$ and F53B $H_{\varepsilon 2}$, G51A $O_{C{=}O}$ and F53B H_{ζ}, G51B $O_{C{=}O}$ and F53A $H_{\delta 1}$, G51B $O_{C{=}O}$ and F53A $H_{\varepsilon 1}$, G51A $O_{C{=}O}$ and F53A $H_{\varepsilon 2}$ (Fig. 8A and B). $CH\cdots\pi$ interactions existed between G48A $H_{\alpha 1}$, G48A $H_{\alpha 2}$ and the phenyl ring of F53B, and between G48B $H_{\alpha 1}$, G48B $H_{\alpha 2}$, I50B $H_{\gamma 1}$ and the phenyl ring of F53A (Table 2). Although, a strong $CH\cdots\pi$ interaction existed between I50A, I50B $H_{\delta 1}$ and the phenyl group of F53A and F53 B, respectively, in the crystal structure, these interactions were only observed in the first 1400 ps. The occurrence of $C_{AR}H\cdots O{=}C$ interactions increased after 1400 ps. The existence of the $C_{AR}H\cdots O{=}C$ interactions indicate that the flaps increased their interaction overlap compared to the semi-open crystal structure.

A conformational transition in the tip of flap A at around 1400 ps resulted in the disappearance of the $CH\cdots\pi$

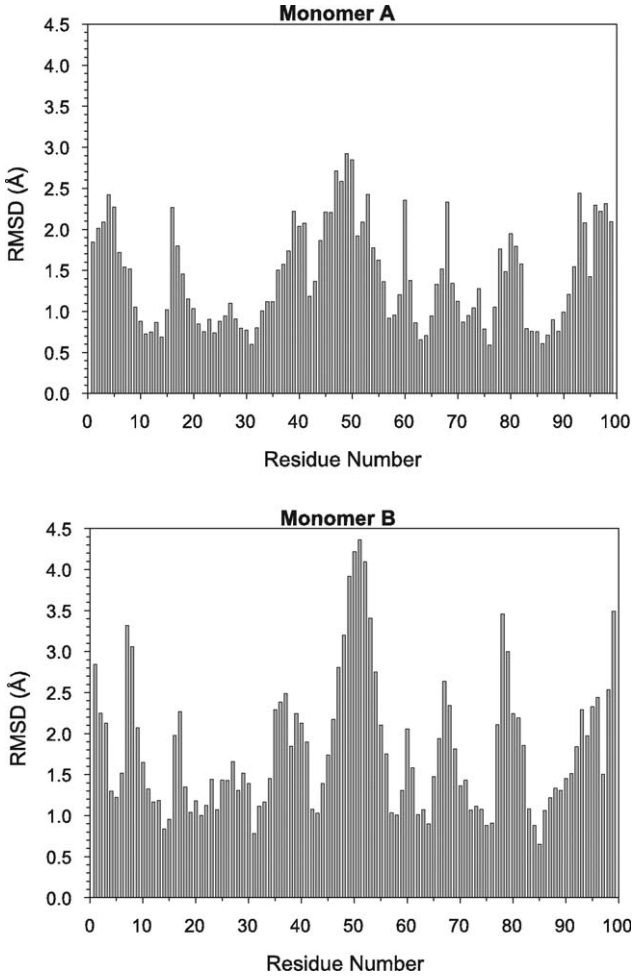

Fig. 4. Average root mean square deviation (RMSD) of the C_α atoms over the 5 ns trajectory between the crystal structure and simulated structures of HIV-1 PR as a function of residue number from the simulation at 296 K.

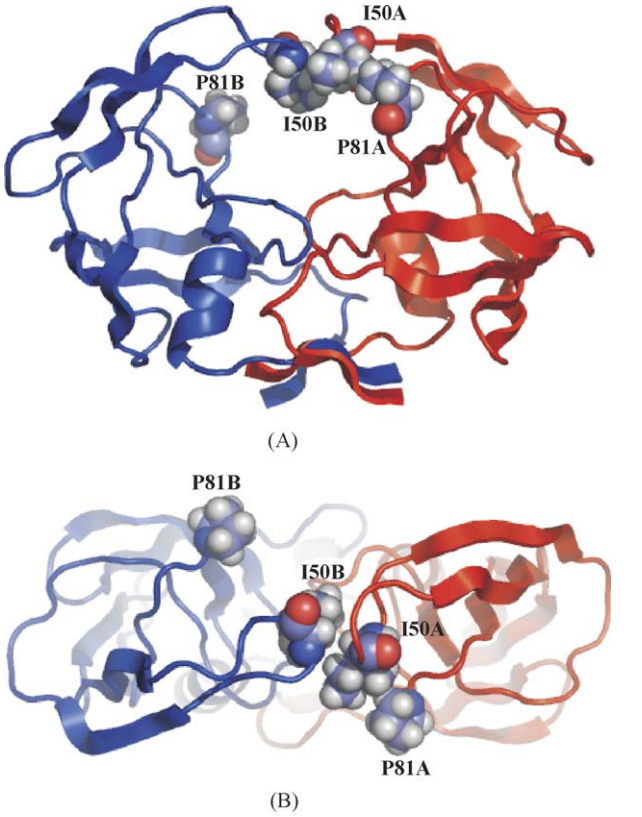

Fig. 5. Cartoon drawing of the hydrophobic cluster between the side chain of I50A and P81A in the asymmetric semi-open flap conformation of ligand free HIV-1 PR. Front (A) and top (B) view. Monomer A is in red, while monomer B is in blue. Selected residues are shown in sphere representation.

interactions between the side chains of Ile50 and the phenyl group of F53 of both monomers, and of the $C_\alpha H\cdots O{=}C$ interactions between F50 $H_{C\alpha}$ and G49 $O_{C=O}$ of both monomers. The tip of flap A was in two conformational states (Table 3). Conformational state I transferred into conformational state II at around 1400 ps. The tip of flap B was in three conformational states (Table 3). Exchanges between conformational states were observed on the 100 ps time scale. These observations suggest that at least two additional conformational states of the flap tips exist in the semi-open conformation of the flaps compared to the crystal structures.

Visual inspection of the semi-open flap conformational families of the protease in surface representation mode suggested that substrate and inhibitor access to the active site

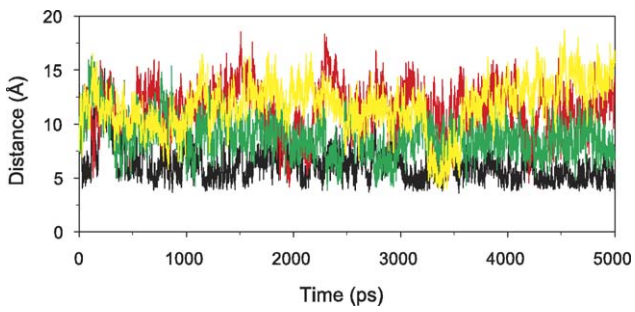

Fig. 6. The evolution of the distance during the simulations between the C_β atom of I50A and the C_γ atom of P81A at 296 K (green line) and at 316 K (black line), and C_β atom of I50B and C_γ atom of P81B at 296 K (yellow line) and at 316 K (red line).

Table 3
Conformational states of the flap tips during the simulation at 296 K

Residue	Conformational state	ϕ (°)	ψ (°)
X-ray (1hhp)			
I50A/Ile50B	I	−57	132
G51A/Gly50B	I	86	−29
MD—monomer A			
I50A	I	−86	112
	II	−133	−10
G51A	I	94	−50
	II	120	49
MD—monomer B			
I50B	I	−86	112
	II	−133	−10
G50B	I	94	−50
	II	120	49
	III	−120	−50/49

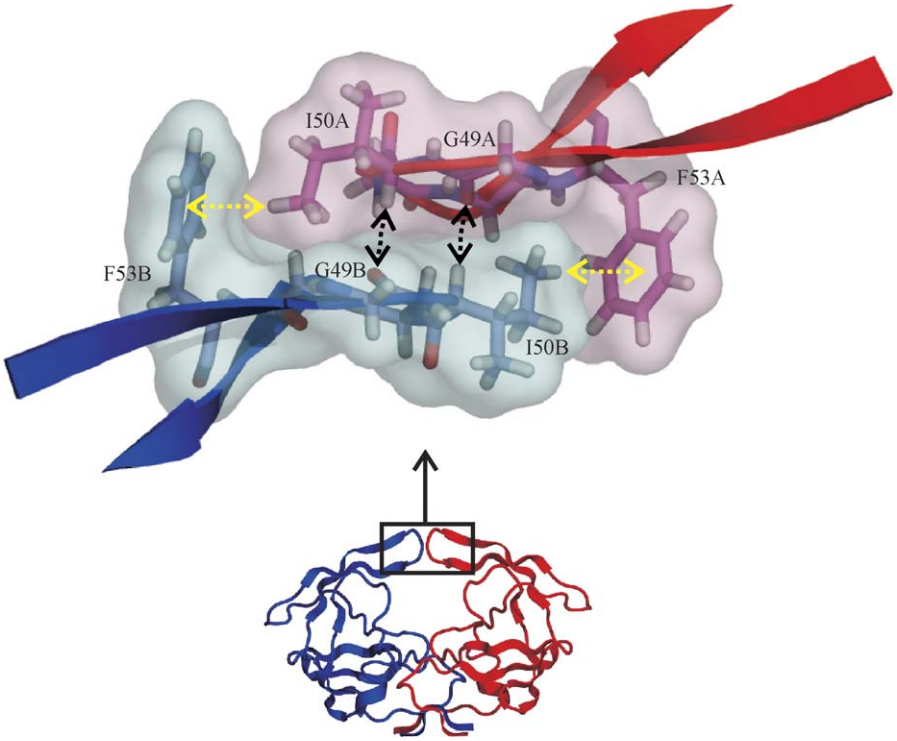

Fig. 7. Selected weakly polar interactions between the two flaps of HIV-1 PR. Residues G49, I50 and F53 of both monomers are shown in both surface and stick representations. Backbone is drawn in cartoon representations: monomer A is in red, while monomer B is in blue. Yellow arrows indicate CH–π interactions, while black arrows indicate CH· · ·O=C interactions.

is not likely in this flap conformation due to the small size of the entrance to the active site.

3.3. Mechanism of flap separation from the semi-open flap conformation of HIV-1 PR

Flap separation happened in two different mechanisms during the simulations. In mechanism one (M1) the separation of the flaps was preceded by the formation of a hydrophobic cluster between the side chains of Ile50 and Pro81 of the same monomer. This cluster was similar to the one observed in the simulations at 296 and 316 K (Fig. 5). It appears that the presence of this cluster promoted the separation of the flaps in an asymmetric way by destabilizing the symmetric flap–flap interaction. M1 was observed in the simulations at 306 and 311 K. In mechanism two (M2), the flaps separated in a symmetric way by the slow disruption of the flap–flap interactions. M2 was observed in the simulations at 301 and 321 K.

The formation of the open flap conformations of HIV-1 PR was observed to be driven by the hydrophobic effect as several key hydrophobic contacts were formed between the flap and the rest of the protease. With the loss of the anchoring flap–flap interactions the flaps were free in movement. The flaps went through a transitional period right after flap separation, when they were intensely mobile, by loosing their β-hairpin structure and forming loop like structures. Occasionally the flap tips formed interactions with nearby hydrophobic residues temporarily. At the end of this transition period, in all four simulations, the formation of a hydrophobic cluster between I50 of both chains and P81 of one of the chains was observed. This hydrophobic cluster will be referred here as intermediate state cluster (Fig. 9). Interestingly, the distance between C_α of I50A and C_α of I50B in the intermediate state cluster was at the minimum during the transition period. These distances were 5.32, 3.99, 5.82, and 6.10 Å at 372, 463, 900, and 334 ps of the trajectories simulated at 301, 306, 311 and 321 K, respectively (Fig. 7). The lifetime of the clusters varied in the simulations from about 4 to 20 ps long. The structure of the intermediate state cluster slightly differed in the simulations. At 306 K the side chain of Pro81A was straddled by the two I50 side chains (Fig. 9A), while at 301, 311 and 321 K the two I50 side chains formed contacts between each other and only one of the I50 had contacts with the side chain of P81 (Fig. 9B). This later intermediate had a similar structure to the one in the semi-open conformation (Fig. 5).

3.4. Structure and dynamics of the HIV-1 PR after flap separation

Flap separation from the semi-open flap conformation resulted in two distinct flap conformational families in HIV-PR. At 301, 306 and 321 K the flaps separation resulted a family of flap conformations often referred to as open flap conformations, while at 311 K it yielded curled flap conformations.

HIV-1 PR with open flap conformations was separated into three distinct conformational families (Fig. 10) on the basis of the conformations of the flaps and their interactions with the rest of the enzyme. Each conformational family can be

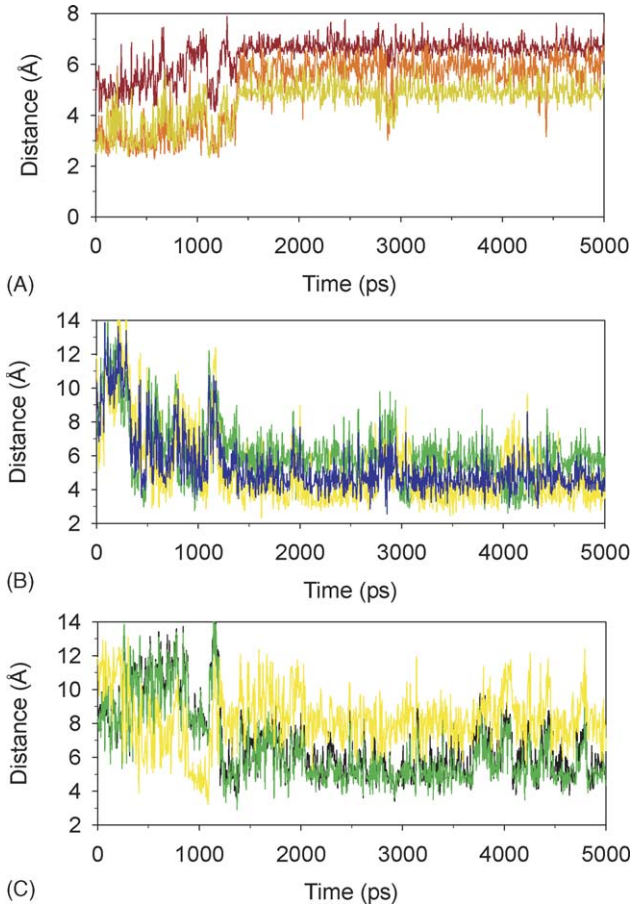

Fig. 8. Distance between (A) I50A C_α and I50B C_α (brown line), G49A $O_{C=O}$ and I50B $H_{C\alpha}$ (orange line), G49B $O_{C=O}$ and I50A $H_{C\alpha}$ (green line); (B) G51A $O_{C=O}$ and F53B $H_{\varepsilon 1}$ (green line), G51A $O_{C=O}$ and F53B $H_{\varepsilon 2}$ (yellow line), G51A $O_{C=O}$ and F53B H_ζ (blue line); (C) G51B $O_{C=O}$ and F53A $H_{\delta 1}$ (black line), G51B $O_{C=O}$ and F53A $H_{\varepsilon 1}$ (green line), G51B $O_{C=O}$ and F53A $H_{\varepsilon 2}$ (yellow line) during the simulation at 296 K.

characterized by the interaction between I50, located at the tip of the flap and certain hydrophobic residues located in the rest of the protease (Table 4). Transition between these conformational families was observed during the simulations. Both the transition and the stability of the conformational families were

Table 4
Main residue contacts in the HIV-1 PR with open flap conformations (simulated)

Conformation	Monomer A	Monomer B
I	I50–P81	I50–V32, I50–V82
II	I50–P81	I50–P81
III	I50–V32, I50–V82	I50–V32, I50–V82

in the 100 ps time scale in our simulations. Visual inspection of the three conformational families of the protease with open flap conformations in surface representation mode indicated that the opening to the active site is large enough for substrate and inhibitor access into the active site.

The curled flap conformation of HIV-1 PR (Fig. 11) was observed to be stable for over 3500 ps during the simulation at 311 K. The curled flap conformation was formed by the curling of tip of the flaps into the active site of HIV-1 PR, where the side chains of I50A and I50B of the flap tips interfaced as they were surrounded by the hydrophobic side chains of the residues I84 and V82 of both chains, V32A and A28A. Visual inspection of curled flap conformations of the protease in surface representation mode suggested that substrate and inhibitor access to the active site is not possible in this flap conformation.

4. Discussion

4.1. Flap conformations of HIV-1 PR

The simulation results of this study provide the most complete description of the dynamics of the flaps in ligand free HIV-1 PR up to date. The results of the study show that the flaps of HIV-1 PR may exist in an ensemble of conformations consisting of semi-open, open and curled conformations. This is consistent with the observation of Freedberg et al. [9], based on their NMR studies and the MD results of Scott and Schiffer [17] and Collins et al. [18], that the flaps may exist in an ensemble of conformations ranging between the semi-open and open conformations.

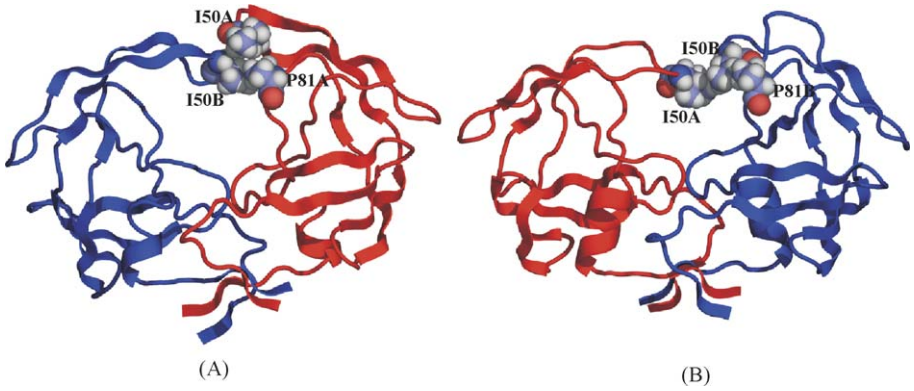

Fig. 9. Cartoon drawing of the intermediate state clusters observed at 301, 306, 311, and 321 K. (A) The side chain of P81A is straddled by the two I50 side chains. (B) Only one of the I50 formed contacts with the P81 side chain, while the two I50 side chains stacked against each other. Monomer A is in red, while monomer B is in blue. Selected residues are shown in sphere representation.

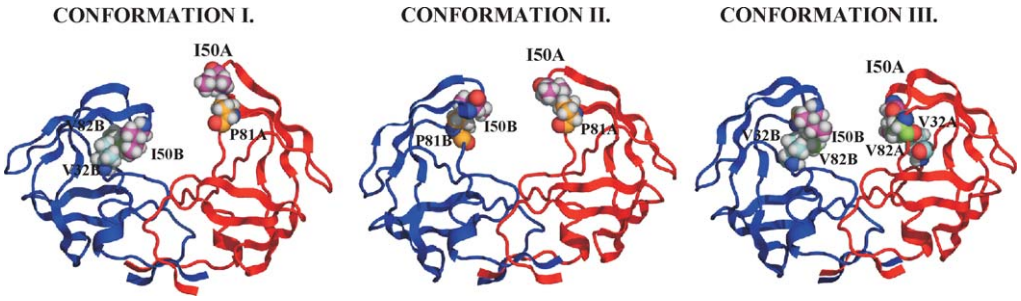

Fig. 10. Cartoon drawing of the conformational families of the HIV-1 PR with open flap conformations. Monomer A is in red, while monomer B is in blue. Selected residues are shown in sphere representation. The carbon atoms of I50 are magenta, of P81 are yellow, of V32 are cyan, and of V82 are green.

The flaps of HIV-1 PR showed complex dynamic behavior during the simulations. The structural basis for flap separation and flap dynamics has been difficult to investigate using experimental techniques at an atomic resolution due to the short timescales associated with their dynamics. Computational techniques such as MD simulations, however, were able to provide details of the mobility and structural changes of the flaps associated with their separation and dynamics. This is well illustrated by the observation of the two mechanisms of flap separation and the various stable flap conformations (semi-open, open and curled) observed during the trajectories.

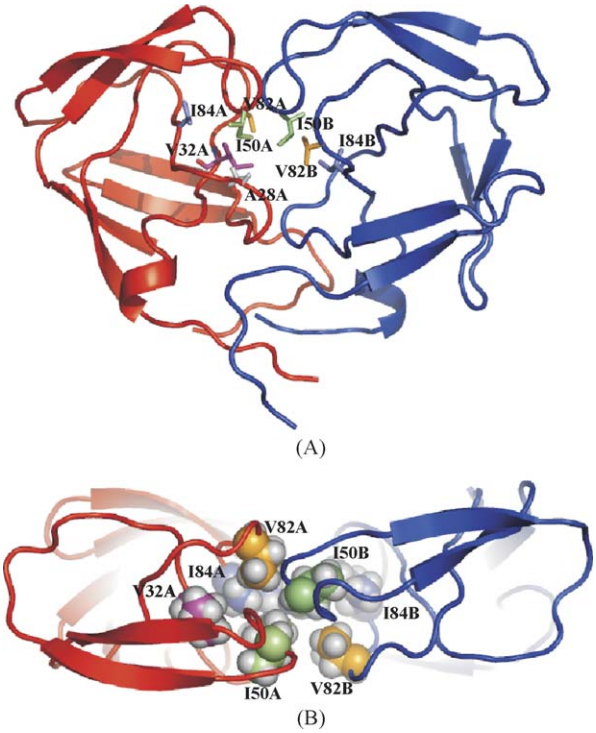

Fig. 11. Cartoon drawing of the curled flap conformation of HIV-1 PR. Front (A) and top (B) view. Monomer A is in red, while monomer B is in blue. Selected residues are shown in stick (hydrogens hidden) (A) and sphere representation (B).

4.2. The role of weakly polar interactions in the stabilization of the semi-open flap conformation of HIV-1 PR

Our results indicate that the network of weakly polar interactions observed between the flaps is responsible for keeping the flaps in the semi-open conformation at 296 and 316 K. It is not likely that any one of the weakly polar interactions could hold the flaps in the semi-open conformation, since the strength of these interactions is generally between −0.5 and −3 kcal/mol in gas phase [38,39]. The observation that several of these weakly polar interactions exist between the flaps at the same time suggests, that such interactions have the ability to synergistically stabilize the semi-open conformation. This is consistent with previous findings where networks of weakly polar interactions were observed to be responsible for the formation of local conformations in peptides and proteins [30], and where Pro-rich motifs are recognized by aromatic side chains in SH3 and WW domains in protein–peptide and protein–protein interactions [40]. On the latter basis, Zarrinpar and Lim [41] suggested that the low affinity interaction between Pro-rich motifs and SH3 and WW domains allow sensitive and dynamic modulation of binding in response to changing signaling conditions. This may also apply to HIV-1 PR, where small external stimuli, for example the proximity of substrate could substantially influence the conformation of the flaps. In the case of the semi-open conformation, such effect could break up the network of weakly polar interactions and cause flap opening. Therefore, the role of weakly polar interactions may be to serve as a sensitive lock on a ‘‘gate’’ formed by the flaps, which control the access to the active site. The case of the flap interactions of HIV-1 PR contributes to the further understanding of the role of weakly polar interactions in biomolecular assemblies.

4.3. The role of the flaps in the binding mechanism of ligands to HIV-1 PR

Fluorescence and NMR studies of the kinetics of the binding mechanism of HIV-1 PR inhibitors [10,42,43] suggested a two-step binding mechanism for HIV-1 inhibitors. The following two models for ligand binding to HIV-1 PR are plausible on the

basis of the two-step binding mechanism. In the first model, the ligand forms a collision complex with HIV-1 PR in open flap conformation as it enters the active site of the protease and then induces the closing of the flaps [17]. Alternatively, in the second model, the proximity of the ligand induces the disruption of flap–flap interactions as the ligand approaches HIV-1 PR in semi-open flap conformation. This causes the flaps to adopt open flap conformations as the ligand enters the active site of the protease. The next step of this second model is the closing of the flaps induced by presence of the ligand in the active site. Both of these models are possible in a two-step binding mechanism, if in the second model the opening of the flaps and active site access of the ligand are one step kinetically. Our simulation results support both models.

4.4. Comparison of the simulations with previous MD simulations

The observation that the flaps of HIV-1 PR open up is consistent with the simulations of Scott and Schiffer [17] and Erickson and co-workers [18]. The timescale of the opening presented in this work differs from the results of previous simulations. This can be attributed to the chaotic nature of MD simulations, difference in simulation temperatures, and/or to the modeling of the viscosity of the system. Previous studies modeled the aqueous environment using an explicit water model [17], while in this study continuum solvation was used with low viscosity setting. It has been shown that at low viscosities the rate of protein folding increases as diffusion times decrease and conformational sampling increases [28]. Therefore, the use of continuum solvation and low viscosity in this study enabled us higher sampling of HIV-1 PR compared to an explicit water simulation in the same time scale, at a lower cost of computational time.

5. Conclusion

In this study the mechanism of flap opening and the structure and dynamics of HIV-1 PR with semi-open and separated flap conformations was investigated using molecular dynamics simulations. Our calculations revealed two distinct mechanisms of flap opening from the semi-open flap conformation of HIV-1 PR. After flap opening three distinct families of HIV-1 PR with open flap conformations and a family of HIV-1 PR with curled flap conformation was observed. A network of weakly polar interactions between the flap tips in the semi-open flap conformation were proposed to be responsible for making flap opening a highly sensitive gating mechanism which controls access to the active site.

Acknowledgment

Thanks to Sia Meshkat and Paolo Carnevali for critical reading of the manuscript. The authors gratefully acknowledge the work of many people at Protein Mechanics and Locus Pharmaceuticals who have contributed to the development of Imagiro.

References

[1] R.A. Katz, A.M. Skalka, Annu. Rev. Biochem. 63 (1994) 133–173.
[2] A. Wlodawer, J. Vondrasek, Annu. Rev. Biophys. Biomol. Struct. 27 (1998) 249–284.
[3] S. Spinelli, Q.Z. Liu, P.M. Alzari, P.H. Hirel, R.J. Poljak, Biochimie 73 (1991) 1391–1396.
[4] R. Lapatto, T. Blundell, A. Hemmings, J. Overington, A. Wilderspin, S. Wood, J.R. Merson, P.J. Whittle, D.E. Danley, K.F. Geoghegan, Nature 342 (1989) 299–302.
[5] A. Wlodawer, M. Miller, M. Jaskolski, B.K. Sathyanarayana, E. Baldwin, I.T. Weber, L.M. Selk, L. Clawson, J. Schneider, S.B. Kent, Conserved folding in retroviral proteases: crystal structure of a synthetic HIV-1 protease, Science 245 (1989) 616–621.
[6] J.M. Louis, F. Dyda, N.T. Nashed, A.R. Kimmel, D.R. Davies, Biochemistry 37 (1998) 2105–2110.
[7] M. Prabu-Jeyabalan, E. Nalivaika, C.A. Schiffer, J. Mol. Biol. 301 (2000) 1207–1220.
[8] R. Ishima, D.I. Freedberg, Y.X. Wang, J.M. Louis, D.A. Torchia, Struct. Fold. Des. 7 (1999) 1047–1055.
[9] D.I. Freedberg, R. Ishima, J. Jacob, Y.X. Wang, I. Kustanovich, J.M. Louis, D.A. Torchia, Protein Sci. 11 (2002) 221–232.
[10] E. Katoh, J.M. Louis, T. Yamazaki, A.M. Gronenborn, D.A. Torchia, R. Ishima, Protein Sci. 12 (2003) 1376–1385.
[11] L.K. Nicholson, T. Yamazaki, D.A. Torchia, S. Grzesiek, A. Bax, S.J. Stahl, J.D. Kaufman, P. Wingfield, T. Lam, P.K. Jadhav, Nat. Struct. Biol. 2 (1995) 274–280.
[12] M. Miller, J. Schneider, B.K. Sathyanarayana, M.V. Toth, G.R. Marshall, L. Clawson, L. Selk, S.B. Kent, A. Wlodawer, Science 246 (1989) 1149–1152.
[13] S.W. Rick, J.W. Erickson, S.K. Burt, Proteins 32 (1998) 7–16.
[14] S. Piana, P. Carloni, U. Rothlisberger, Protein Sci. 11 (2002) 2393–2402.
[15] Y. Levy, A. Caflisch, J. Phys. Chem. B 107 (2003) 3068–3079.
[16] A.L. Perryman, J.H. Lin, J.A. McCammon, Protein Sci. 13 (2004) 1108–1123.
[17] W.R. Scott, C.A. Schiffer, Struct. Fold. Des. 8 (2000) 1259–1265.
[18] J.R. Collins, S.K. Burt, J.W. Erickson, Nat. Struct. Biol. 2 (1995) 334–338.
[19] A.F. Wilderspin, R.J. Sugrue, J. Mol. Biol. 239 (1994) 97–103.
[20] R.B. Rose, C.S. Craik, R.M. Stroud, Biochemistry 37 (1998) 2607–2621.
[21] B. Pillai, K.K. Kannan, M.V. Hosur, Proteins 43 (2001) 57–64.
[22] P. Carnevali, G. Toth, G. Toubassi, S.N. Meshkat, J. Am. Chem. Soc. 125 (2003) 14244–14245.
[23] G.R.A.F. Kaminski, J. Tirado-Rives, W.L. Jorgensen, J. Phys. Chem. B 105 (2001) 6474–6487.
[24] W.C.T.A. Still, R.C. Hawley, T. Hendrickson, J. Am. Chem. Soc. 112 (1990) 6127–6129.
[25] V. Katritch, M. Totrov, R. Abagyan, J. Comput. Chem. 24 (2003) 254–265.
[26] P. Underwood, Dynamic relaxation, in: T. Belytschko, T.J.R. Hughes (Eds.), Computational Methods for Transient Analyses, Elsevier Science Publishers B.V., 1983, pp. 245–265.
[27] J.C. Butcher, The Numerical Analysis of Ordinary Differential Equations: Runge–Kutta and General Linear Methods, Wiley, Chichester, 1987.
[28] B. Zagrovic, V. Pande, Solvent viscosity dependence of the folding rate of a small protein: distributed computing study, J. Comput. Chem. 24 (2003) 1432–1436.
[29] F. Nardi, J. Kemmink, M. Sattler, R.C. Wade, J. Biomol. NMR 17 (2000) 63–77.
[30] G. Toth, R.F. Murphy, S. Lovas, Protein Eng. 14 (2001) 543–547.
[31] P.W. Williamson, T.J. Asakura, Empirical comparisons of models for chemical-shift calculations in proteins, J. Magn. Reson., Ser. B 101 (1993) 67–71.
[32] P. Chakrabarti, S. Chakrabarti, J. Mol. Biol. 284 (1998) 867–873.
[33] W.L. DeLano, The PyMOL User's Manual, Delano Scientific, San Carlos, USA, 2002.

[34] S.K. Burley, G.A. Petsko, Adv. Protein Chem. 39 (1988) 125–189.
[35] P. Hobza, Z. Havlas, Chem. Rev. 100 (2000) 4253–4264.
[36] Z.S. Derewenda, L. Lee, U. Derewenda, J. Mol. Biol. 252 (1995) 248–262.
[37] M. Nishio, Y. Umezawa, M. Hirota, Y. Takeuchi, Tetrahedron 51 (1995) 8665–8701.
[38] E.A. Meyer, R.K. Castellano, F. Diederich, Angew. Chem. Int. Ed. Engl. 42 (2003) 1210–1250.
[39] R. Vargas, J. Garza, R.A. Friesner, H. Stern, P.B. Hay, A.D. Dixon, J. Phys. Chem. B 105 (2001) 4963–4968.
[40] R. Bhattacharyya, P. Chakrabarti, J. Mol. Biol. 331 (2003) 925–940.
[41] A. Zarrinpar, W.A. Lim, Nat. Struct. Biol. 7 (2000) 611–613.
[42] E.S. Furfine, E.D. Souza, K.J. Ingold, J.J. Leban, T. Spector, D.J. Porter, Biochemistry 31 (1992) 7886–7891.
[43] E.J. Rodriguez, C. Debouck, I.C. Deckman, H. Abu-Soud, F.M. Raushel, T.D. Meek, Biochemistry 32 (1993) 3557–3563.